

Supporting Information

Malashkevich et al. 10.1073/pnas.0913660107

SI Text

SI Methods. Structure determination. Recombinant human S100A4 was purified as described previously (1). S100A4 in 20 mM Tris pH 7.5, 20 mM KCl, 10 mM DTT, 20 mM CaCl₂, and 0.02% NaN₃ was concentrated to 20–30 mg/mL (~0.85–1.28 mM dimer) and trifluoperazine (TFP) or prochlorperazine (PCP) was added to a concentration of 5 mM (final DMSO 2%) or 1 mM (final dioxane 4%), respectively. Diffraction quality crystals of Ca²⁺-S100A4/TFP were obtained by hanging drop vapor diffusion at 21 °C by mixing 1 μL of S100A4/TFP with 1 μL of reservoir solution containing 0.1 M Hepes, pH 7.0 and 30% v/v Jeffamine ED-2001 and equilibrating the samples against reservoir solution for 1–2 weeks. Diffraction from these crystals is consistent with the space group P2₁ with unit cell dimensions $a = 108.79 \text{ \AA}$, $b = 102.49 \text{ \AA}$, $c = 116.63 \text{ \AA}$, $\beta = 92.59^\circ$ and twenty S100A4 chains in the asymmetric unit.

Diffraction quality crystals of Ca²⁺-S100A4/PCP were obtained by hanging drop vapor diffusion at 21 °C by mixing 1 μL of S100A4/PCP with 1 μL of reservoir solution containing 0.2 M ammonium sulfate, 0.1 M Tris pH 7.5, 20% w/v PEG-monomethyl ether (MME) 5000 and equilibrating the samples against reservoir solution for 23 weeks. Diffraction from these crystals is consistent with the space group P2₁ with unit cell dimensions $a = 54.58 \text{ \AA}$, $b = 102.28 \text{ \AA}$, $c = 117.37 \text{ \AA}$, $\beta = 92.6^\circ$ and ten S100A4 chains in the asymmetric unit. The unit cells of the two S100A4 inhibitor complexes are very similar; however, in the S100A4/TFP complex the a axis is twice as long. The S100A4/TFP crystals demonstrate strong pseudo translational symmetry along the a axis and systematic near absences of odd reflections at low resolution, but at higher resolution the larger unit cell is apparent.

Crystals in mother liquor were flash-cooled in liquid nitrogen. For Ca²⁺-S100A4/TFP crystals, diffraction data were collected at the LRL-CAT beamline (Advanced Photon Source, Argonne, USA) using an MAR-165 charge-coupled device (CCD) detector and 0.979 Å wavelength radiation. For Ca²⁺-S100A4/PCP crystals, diffraction data were collected at the X-29 beamline (National Synchrotron Light Source in Brookhaven National Laboratory) using a Quantum-315 CCD detector and 1.073 Å wavelength radiation. Intensities were integrated using HKL2000 and reduced to amplitudes with TRUNCATE (2 and 3). The structures of the S100A4/TFP and S100A4/PCP complexes were determined by molecular replacement to 2.3 Å and 2.7 Å, respectively using the program PHASER (4) and the structure of the Ca²⁺-S100A4 (PDB 2Q91, (5)) as the search model. Model building and refinement were performed using REFMAC and COOT (3 and 6). The quality of the final structure was verified with composite omit maps, and the stereochemistry was checked with WHATCHECK (7) and PROCHECK (8).

The final Ca²⁺-S100A4/TFP model contained 20 subunit chains of 94 residues each (Ala2 to Pro95), 40 calcium ions, 40 TFP molecules, and 1,228 water molecules with an $R_{\text{cryst}}/R_{\text{free}}$ of 0.206/0.259 (PDB entry 3KO0). The final Ca²⁺-S100A4/PCP model contained 10 subunit chains of 94 residues each (Ala2 to Pro95), 20 calcium ions, 10 PCP molecules, and 11 water molecules with an $R_{\text{cryst}}/R_{\text{free}}$ of 0.238/0.310 (PDB entry 3M0W). The LSQKAB and secondary-structure matching (SSM) algorithms were used for structural superimpositions (3 and 9). Quaternary structure and accessible surface areas were analyzed using the PISA server.

NMR spectroscopy. The Ca²⁺-S100A4 NMR samples contained 0.35 mM S100A4 subunit, 0.34 mM NaN₃, 0–100 μM TFP, 15 mM NaCl, 10 mM CaCl₂, 10% D₂O, and 10 mM MES buffer,

pH 6.5. The chemical shift assignments for Ca²⁺-S100A4 were used as the starting point during titrations with TFP to assign the two-dimensional ¹H-¹⁵N HSQC spectra of S100A4 in the TFP-S100A4 complex. At the end of the two-dimensional HSQC titration, a three-dimensional ¹⁵N-edited NOESY-HSQC experiment was performed to unambiguously confirm the assignments. Heteronuclear single quantum coherence NMR data were collected at 37 °C with a Bruker Avance III 600 (600.13 MHz for protons) or with an Avance 800 US2 (800.27 MHz for protons) NMR spectrometer both equipped with pulsed-field gradients, four frequency channels, and triple resonance, z-axis gradient cryogenic probes. Data were processed with NMRPipe (10), and proton chemical shifts were reported with respect to the H₂O or HDO signal taken as 4.658 ppm relative to external TSP (0.0 ppm). The ¹⁵N chemical shifts were indirectly referenced as previously described using the following ratio of the zero-point frequency: 0.10132905 for ¹⁵N to ¹H (11 and 12)

Promotion of disassembly assays. Promotion of disassembly assays were performed with 3 μM S100A4 dimer, 3 μM myosin-IIA rod dimers, and 0–100 μM TFP in 20 mM Tris-HCl pH 7.5, 150 mM NaCl, 1 mM DTT, 2 mM MgCl₂, 0.3 mM CaCl₂, 0.02% NaN₃, and 2% DMSO as described previously (1).

Chemical cross-linking of S100A4-inhibitor complexes. 3 μM S100A4 dimer was incubated for 1 h at room temperature in 20 mM Tris-HCl or 20 mM Hepes pH 7.5, 150 mM NaCl, 1 mM DTT, 2 mM MgCl₂, 0.3 mM CaCl₂, 0.02% NaN₃, and 2% DMSO. For experiments performed in the presence of EGTA the final concentration was 4 mM. The final phenothiazine concentration was approximately twofold higher than the IC₅₀ for inhibition of the Ca²⁺-induced fluorescence increase of the S100A4 biosensor (100 μM trifluoperazine, fluphenazine or prochlorperazine, 200 μM flupenthixol, or 500 μM chlorprothixene or perphenazine) (13). Disuccinimidylsuberate (DSS) (Pierce) was added to final concentration of 5 mM and the reactions were incubated for an additional hour at room temperature. The reaction was quenched by the addition of 5X sample buffer and heating.

Analytical ultracentrifugation. S100A4 was dialyzed into a buffer containing 20 mM Tris pH 7.5, 150 mM KCl, 1 mM tris(2-carboxyethyl)phosphine (TCEP), 0.02% NaN₃, and either 2 mM EDTA and 2 mM EGTA (Ca²⁺-free) or 10 mM CaCl₂ (Ca²⁺-bound). Sedimentation equilibrium experiments were performed using six channel centerpieces with 80 μM S100A4 subunit and 5–500 μM TFP (final DMSO 2%) at 25 °C. For centrifugation studies of crosslinked S100A4-TFP complexes, a 10 mL cross-linking reaction was performed as described above except that 1 mM TCEP was used instead of DTT and the final DSS concentration was 2.75 mM. The reaction was clarified by centrifugation for 15 min at 14,000 × g and the crosslinked sample was concentrated to 80 μM S100A4 subunit. The sample was dialyzed against 20 mM Tris-HCl pH 7.5, 150 mM NaCl, 1 mM TCEP, and 0.02% NaN₃ to remove free DSS. The experiments were performed with 13.3, 40, and 80 μM S100A4 subunit as described above.

Sedimentation profiles were monitored at 280 nanometers. Absorbance scans obtained following 24 h equilibrations at 15,000 and 22,000 rpm (TFP titrations) or 8,000 and 13,000 rpm (S100A4/TFP crosslinked complexes) in a Ti60 rotor (Beckman Coulter, Brea, CA) were globally analyzed using HeteroAnalysis v1.0.114 (Cole, J.L. and Lary, J.W., Analytical Ultracentrifugation Facility,

Biotechnology Services Center, University of Connecticut, Storrs, CT) to obtain the weight-average molecular weight of the S100A4 oligomers. The \bar{v} value of 0.7346 was calculated from the amino acid composition of the wild-type S100A4. Density and viscosity values were provided by Sednterp v1.06 (Hayes, B., Laue T. and Philo, J. (2003), *Sedimentation Interpretation Program*, University of New Hampshire). The calculated mass of the wild-type S100A4 subunit is 11,597 Da. The titration data were plotted as a function of the TFP concentration and fit to the Hill equation to evaluate the midpoint and slope of the curve for S100A4 oligomerization. The best-fit parameters and their 95% joint confidence intervals are reported.

1. Li ZH, Spektor A, Varlamova O, Bresnick AR (2003) Mts1 regulates the assembly of nonmuscle myosin-IIA. *Biochemistry* 42:14258–14266.
2. Otwinowski W, Minor F (1997) Processing of X-ray diffraction data collected in oscillation mode. *Methods Enzymol.* 276:307–326
3. Collaborative Computational Project N (1994) The CCP4 suite: programs for protein crystallography. *Acta Crystallogr D* 50:760–763.
4. Storoni LC, McCoy AJ, Read RJ (2004) Likelihood-enhanced fast rotation functions. *Acta Crystallogr D* 60:432–438.
5. Malashkevich VN, et al. (2008) Structure of Ca²⁺-bound S100A4 and its interaction with peptides derived from nonmuscle myosin-IIA. *Biochemistry* 47:5111–5126.
6. Emsley P, Cowtan K (2004) COOT: model-building tools for molecular graphics. *Acta Crystallogr D* 60:2126–2132.
7. Hoofst RW, Vriend G, Sander C, Abola EE (1996) Errors in protein structures. *Nature* 381:272.
8. Laskowski R, MacArthur M, Moss D, Thornton J (1993) PROCHECK: a program to check the stereochemical quality of protein structures. *J Appl. Cryst.* 26:283–291.
9. Krissinel E, Henrick K (2004) Secondary-structure matching (SSM), a new tool for fast protein structure alignment in three dimensions. *Acta Crystallogr D* 60:2256–2268.
10. Delaglio F, et al. (1995) NMRPipe: a multidimensional spectral processing system based on UNIX pipes. *J Biomol. NMR* 6:277–293.
11. Live DH, Davis D, Agosta W, Cowburn D (1984) Long range hydrogen bond mediated effects in peptides: nitrogen-15 NMR study of gramicidin 5 in water and organic solvents. *Journal of the American Chemical Society* 106:1939–1941.
12. Edison AS, Abildgaard F, Westler WM, Mooberry ES, Markley JL (1994) Practical introduction to theory and implementation of multinuclear, multidimensional nuclear magnetic resonance experiments. *Methods Enzymol.* 239:3–79.
13. Garrett SC, et al. (2008) A biosensor of S100A4 metastasis factor activation: inhibitor screening and cellular activation dynamics. *Biochemistry* 47:986–996.
14. Dulyaninova NG, Malashkevich VN, Almo SC, Bresnick AR (2005) Regulation of myosin-IIA assembly and Mts1 binding by heavy chain phosphorylation. *Biochemistry* 44:6867–6876.

S100A4/myosin-IIA model. The S100A6/SIAH-1 interacting protein peptide complex (PDB 2JTT) was used to build the S100A4/myosin-IIA model. The model structure of the myosin-IIA coiled-coil (residues 1,730–1,928) (14) was unwound at the C terminus to allow single peptide interactions with each S100A4 subunit. The S100A4 binding domain on myosin-IIA (residues 1,908–1,923) (1 and 5) was aligned with the bound peptide in the 2JTT structure so that the hydrophobic residues of the myosin-IIA coiled-coil (i.e., heptad positions *a* and *d*) interacted with the hydrophobic cleft formed by helices 3 and 4 on S100A4. The myosin-IIA heavy chain was bent similarly to the SIAH-1 peptide to maximize interactions with residues exhibiting chemical shift perturbation upon myosin-IIA peptide binding (5).

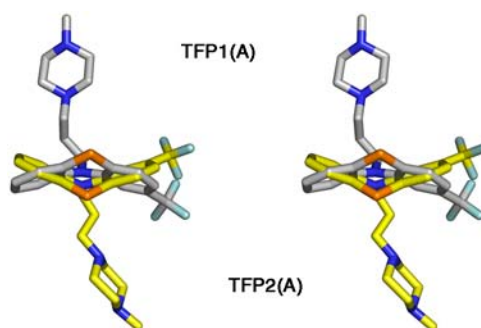


Fig. S1. Stereo image of TFP1(A) superimposed on TFP2(A) (yellow). The piperazine rings have opposite orientations relative to the superimposed phenothiazine moieties.

Table S2. Molecular contacts of bound TFP molecules *

Primary interactions with the target S100A4 molecule

	Subunit A	Subunit B
TFP1(A)	Ser44(A), Phe45(A), Leu46(A), Gly47(A), Ile82(A), Met85(A), Cys86(A), Phe89(A), TFP2(A), 3 water molecules	none
TFP2(A)	Leu42(A), Ser44(A), Phe45(A), Ile82(A), Cys86(A), Phe89(A), TFP1(A), 8 water molecules	Glu6(B), Leu9(B), Asp10(B)
Secondary interactions with symmetry-related molecules		
	Subunit C	Subunit D
TFP1(A)	Phe89(C), Phe90(C), Gly92(C), Phe93(C), TFP1(C)	none
TFP2(A)	Cys86(C), Phe89(C), TFP2(C)	Asp10(D), Ser14(D)

*Calculated with the program CONTACTS using a 4 Å cutoff.

Table S3. Contact area of bound TFP molecules

	TFP1(A)	TFP2(A)
Surface accessible area (Å ²) *	578	574
Change due to binding to:		
Ca ²⁺ -S100A4	-299	-307
Ca ²⁺ -S100A4/TFP1(A)	-	-337
Ca ²⁺ -S100A4/TFP2(A)	-335	-
Symmetry-related molecules	-170	-228
Whole pentamer-of-dimers	-467	-502

*Calculated with the program AREAIMOL.